

High-frequency conductivity of superlattices with electron-phonon coupling

Narkis Tzoar and Chao Zhang

Department of Physics, City College of New York, New York, New York 10031

(Received 14 July 1986)

The high-frequency and long-wavelength conductivity due to electron—optical-phonon interaction was derived for superlattices made out of polar or partially polar semiconductors. The treatment for conductivity rests on Kubo's formula for the conductivity and the temperature-dependent Green's-function formalism. General expressions for the conductivity and the resistivity have been derived, and we have performed numerical calculations for a simple model in which the subband structures of the phonons are ignored and the electronic wave function is approximated by a periodic array of two-dimensional electron gases.

I. INTRODUCTION

Superlattices are a novel class of material composed of alternating layers of two different constituents.¹⁻⁴ The development of molecular-beam epitaxy has made it possible to produce high-quality superlattices made from two different semiconducting materials (e.g., InAs-GaSb, GaAs-AlAs, Ge-GaAs, etc.) with similar lattice structure and matching lattice parameters. In the direction of superlattice growth (called the superlattice axis, and taken to be the z direction), a number of atomic monolayers of semiconductor A are deposited in an atomically sharp way on atomic monolayers of semiconductor B to form new superlattice unit cells. A microscopic sample of such an A - B superlattice is a new bulk material with properties intermediate between those of materials A and B .

There are two types of superlattices whose properties have been studied in some detail. These are known as type-I and type-II superlattices. Type-I superlattices are typified by the GaAs- $\text{Al}_x\text{Ga}_{1-x}\text{As}$ system, in which the band gap of GaAs is smaller than, and contained within, that of $\text{Al}_x\text{Ga}_{1-x}\text{As}$, giving rise to band-gap discontinuities in both conduction and valence bands of the resultant superlattice system. If we dope the $\text{Al}_x\text{Ga}_{1-x}\text{As}$ layers with donor impurities, electrons will be released from the donors to drop into the GaAs sides of the band-gap discontinuities. The resulting one-dimensional potential well quantizes the motion of the electron in the z direction, and so the conduction band of GaAs will be split up into a series of subbands (if the electron wave functions in adjacent potential wells do not overlap) or miniband (if they do), each of which represents a continuum of free-electron-like states in the x - y plane. Thus, as far as electronic properties are concerned, type-I superlattices consist of a periodic array of quasi-two-dimensional electron gases. Many aspects of type-I superlattices, such as dielectric response, collective excitations, cyclotron resonance, and Raman scattering, have been studied⁵⁻¹² in recent years.

A type-II superlattice is typified by InAs-GaSb. The band discontinuities at the interfaces are so large that the conduction-band edge in InAs lies below the upper valence-band edge of the GaSb.¹³ In this case, there is a

transfer of electrons from one layer (GaSb) to the other (InAs), resulting in a spatial separation of electrons and holes into potential wells, with the formation of electron and hole subbands. Unlike type-I superlattices where both electron or hole states are primarily in the GaAs regions, here electrons mainly exist in the InAs layers while the holes are in the GaSb layers.¹⁴⁻¹⁶

The spatial separation of the superlattice system has obvious consequences for the optical properties such as absorption. The mobility of this structure is higher than that of bulk material because of a reduction in the electron-impurity or electron-hole scattering. We have previously reported calculations of the conductivity of type-I and type-II superlattices^{17,18} where the frequency-dependent effective mass and scattering time due to the electron-impurity interaction or the electron-hole interaction were obtained. In this paper we shall calculate the high-frequency conductivity of superlattice systems due to the electron—LO-phonon interaction. Many of these semiconductor superlattices are made of weakly polar III-V or II-VI compound semiconductor materials (e.g., GaAs- $\text{Al}_x\text{Ga}_{1-x}\text{As}$ and InAs-GaSb). In view of the two-dimensional electron confinement in these systems, one expects that the effects of the electron—LO-phonon coupling on the absorption properties will be important. In fact, a number of theoretical¹⁹⁻²⁵ and experimental works²⁶⁻³¹ have already been done in various aspects of the electron-LO-phonon interaction effects on the polarons and electronic properties of two-dimensional systems.

We use the Kubo's formula for conductivity and the temperature-dependent Green's-function technique. We restrict ourselves to the approximation that electrons are confined in sheets of zero thickness. If the energy of the incident photons is less than the energy difference between the ground state and the first excited state, and the mean spreading of wave function is less than the layer thickness, our approximation is realistic and can be used as a model for theoretical calculation which should be valid in and can be compared with real systems. Within this model, we have obtained an exact expression for the conductivity. It is dependent on frequency, plasma parameter r_s , spatial separation a , and the electron-LO-phonon coupling. We have evaluated the relaxation time numerically

for a weakly interacting polar system (GaAs-Ga_{1-x}GaAl_xAs) as well as a strongly interacting polar system (PbTe-Pb_{1-x}Sn_xTe).

The model we use is simple: A purely two-dimensional confined electron gas interacts via the Frohlich Hamiltonian with the bulk LO phonons of the relevant semiconductor material. Here we neglect coupling to all other kinds of phonons as well as to interface phonon. We have two reasons for ignoring the effects of the interface phonons. One is experimental—light scattering experiments³² seem to indicate that the bulk LO phonons are the only phonons that couple to the two-dimensional confined electrons. The second one is theoretical—the superlattice system that we are considering consist of two lattice-matched semiconductors (e.g., GaAs and Al_xGa_{1-x}As) with rather similar lattice dielectric properties which make the existence of purely interface phonon modes (with their own distinct frequencies) rather unlikely.¹⁹

II. EVALUATION OF THE CONDUCTIVITY

Let us consider electrons of density n per unit area and mass m occupying layers positioned at $z=la$ ($l=0, \pm 1, \pm 2, \dots$) where a is the period of the superlattice system along z direction. We use a simplified model in which electrons can only move in the x - y plane. The wave function of the electron in l th layer is

$$\phi_l(\mathbf{p}, \mathbf{r}, z) = e^{i\mathbf{p} \cdot \mathbf{r}} \xi_l(z - la), \quad (2.1)$$

where \mathbf{p}, \mathbf{r} are, respectively, the two-dimensional (2D) momentum and position vector along the x - y plane. $\xi_l(z)$ is defined in such a way that it gives δ -function-like distribution:

$$|\xi_l(z)|^2 = \delta(z - la). \quad (2.2)$$

The Hamiltonian of our electron-phonon system is given as

$$H = H_0 + H_1, \quad (2.3)$$

where

$$H_0 = \sum_{\mathbf{p}, l} E_p a_{\mathbf{p}, l}^\dagger a_{\mathbf{p}, l} + \sum_{\mathbf{Q}} \omega_{\mathbf{Q}} b_{\mathbf{Q}}^\dagger b_{\mathbf{Q}}, \quad (2.4)$$

where $\mathbf{Q} = (\mathbf{q}, q_z)$ is a three-dimensional vector because our two-dimensional electron gas only interact with the bulk phonon of the compound, and

$$H_1 = \frac{1}{2} \sum_{\mathbf{q}, \mathbf{p}, l} \sum_{l', l''} V_q e^{-q|l-l'|} a_{\mathbf{p}+\mathbf{q}, l}^\dagger a_{\mathbf{p}-\mathbf{q}, l'}^\dagger a_{\mathbf{p}, l''} + \sum_{\mathbf{Q}, l} C_l(\mathbf{q}, q_z) a_{\mathbf{p}-\mathbf{q}, l}^\dagger a_{\mathbf{p}, l} (b_{\mathbf{Q}}^\dagger + b_{-\mathbf{Q}}). \quad (2.5)$$

Here $E_p = p^2/2m$ is the kinetic energy of an electron having momentum \mathbf{p} . $\omega_{\mathbf{Q}}$ is the wave-number-dependent longitudinal-optical frequency and $a_{\mathbf{p}, l}^\dagger a_{\mathbf{p}, l} (b_{\mathbf{Q}}^\dagger, b_{\mathbf{Q}})$ represent, respectively, the electron (phonon) creation and destruction operators with momentum $\mathbf{p}(\mathbf{Q})$ in the l th layer. The coupling term $V_q = 2\pi e^2/q\epsilon_\infty$ is the Fourier transform of the Coulomb interaction for planar electrons. The coupling between planar electron and bulk LO

phonon is

$$C_l(\mathbf{q}, q_z) = i \left[\frac{2\pi e^2 \omega_{\text{LO}}}{(q^2 + q_z^2)} \left(\frac{1}{\epsilon_\infty} - \frac{1}{\epsilon_0} \right) \right]^{1/2} \times \int dz e^{iq_z z} \xi_l(z) \xi_l^*(z). \quad (2.6)$$

For δ -function distribution, Eq. (2.6) simply becomes

$$C_l(\mathbf{q}, q_z) = i \left[\frac{2\pi e^2 \omega_{\text{LO}}}{(q^2 + q_z^2)} \left(\frac{1}{\epsilon_\infty} - \frac{1}{\epsilon_0} \right) \right]^{1/2} e^{iq_z la}, \quad (2.7)$$

where ω_{LO} is the longitudinal-optical phonon frequency at zero wave number and $\epsilon_\infty, \epsilon_0$ are, respectively, the high-frequency and static dielectric constants of the relevant semiconductors.

To evaluate the conductivity, we start from Kubo's³³ formula for conductivity which reads

$$\sigma_{\mu\nu}(\omega) = \int_0^\infty e^{i\omega t} dt \int_0^\beta \langle j_\mu(t - i\lambda) j_\nu(0) \rangle d\lambda, \quad (2.8)$$

where ω is the frequency of electromagnetic wave and we set \hbar equal to unity for notational convenience. Here

$$j_\mu(t) = e^{iHt} j_\mu(0) e^{-iHt} \quad (2.9)$$

is the current operator in Heisenberg representation and the average of an operator is defined by

$$\langle O \rangle = \text{Tr} \left\{ \exp \left[\beta \left(\Omega + \sum_s \mu_s N_s - H \right) \right] O \right\}, \quad (2.10)$$

where H is the total Hamiltonian of the system and Ω is defined by

$$e^{-\beta\Omega} = \text{Tr} \left\{ \exp \left[\beta \left(\sum_s \mu_s N_s - H \right) \right] \right\}. \quad (2.11)$$

In Eqs. (2.10) and (2.11) μ_s and N_s are, respectively, the chemical potential and number operator of s species in the system, and β the inverse of the temperature in energy units. In order to render Eq. (2.8) in a more convenient form we integrate it by parts and obtain

$$\sigma_{\mu\nu}(\omega) = \sigma_{\mu\nu}^0(\omega) + \sigma_{\mu\nu}^1(\omega), \quad (2.12)$$

where

$$\sigma_{\mu\nu}^0(\omega) = -\frac{1}{i\omega} \int_0^\beta d\lambda \langle j_\mu(-i\lambda) j_\nu(0) \rangle = \frac{ie^2}{\omega} \frac{n}{m} \delta_{\mu\nu} \quad (2.13)$$

and

$$\sigma_{\mu\nu}^1(\omega) = \frac{1}{\omega} \int_0^\infty dt e^{i\omega t} \langle [j_\mu(t), j_\nu(0)] \rangle. \quad (2.14)$$

In Eq. (2.13) the square brackets denote the commutator. By this the current operator can be expressed as

$$\mathbf{j}(k) = \frac{e}{m} \sum_{\mathbf{p}, l} \mathbf{p} a_{\mathbf{p}+\mathbf{k}, l}^\dagger a_{\mathbf{p}, l}. \quad (2.15)$$

Calculation of the current-current correlations and the conductivity in the three-dimensional case have been worked out in much detail and are well documented.³⁴ We evaluate the conductivity treating electron-phonon collision within the Born approximation (high-frequency conductivity), however, treating the self-consistent field of the fluctuating electron gas and phonons exactly in the random-phase approximation. Under these approximations, we consider the class of diagrams of Figs. 1(a)–1(e). Our expression includes the full dynamical screening of the electron-phonon systems. The wavy line in Figs. 1(a)–1(e) is the effective interaction of an electron in l th layer with an electron l' th layer which is determined by following integral equation [Fig. 1(f)]

$$\begin{aligned} v_{ll'}(q, \alpha_m) &= V_{ll'}(q) + \sum_{q_z} C_l(q, q_z) C_{l'}^*(q, q_z) D_Q(\alpha_m) \\ &\quad + \sum_{q_z, l_1} C_l(q, q_z) C_{l_1}^*(q, q_z) D_Q(\alpha_m) \\ &\quad \quad \times Q(q, \alpha_m) v_{l_1 l'}(q, \alpha_m) \\ &\quad + \sum_{l_1} V_{ll_1} Q(q, \alpha_m) v_{l_1 l'}(q, \alpha_m), \end{aligned} \quad (2.16)$$

where

$$V_{ll'}(q) = \frac{2\pi e^2}{q \epsilon_\infty} e^{-q|l-l'|a} \quad (2.17)$$

and

$$a_m = \frac{2\pi m i}{\beta}; \quad m = 0, \pm 1, \pm 2, \dots \quad (2.18)$$

In Eq. (2.16), $Q_s(q, \alpha_m)$ is the density fluctuation of 2D electron gas which is independent of layer index given by

$$Q(q, \alpha_m) = \frac{1}{4\pi^2} \int dp \frac{f_{p+q} - f_p}{E_{p+q} - E_p - \alpha_m}. \quad (2.19)$$

Here f_p is the Fermi distribution function,

$$f_p = \frac{1}{\exp(\beta E_p - \beta \mu) + 1}, \quad (2.20)$$

and $D_Q(\alpha_m)$ is the free-phonon propagator,

$$D_Q(\alpha_m) = \frac{\omega_Q}{\alpha_m^2 - \omega_Q^2}. \quad (2.21)$$

Since the momentum transfer q is of order of the Fermi momentum which in turn is much smaller than lattice momentum, we ignore entirely the dispersion of the phonons and replace ω_Q by ω_{LO} :

$$D_Q(\alpha_m) = D(\alpha_m) = \frac{\omega_{LO}}{\alpha_m^2 - \omega_{LO}^2}. \quad (2.22)$$

Therefore, the summation over q_z in Eq. (2.16) can be carried out, and we obtain

$$\begin{aligned} v_{ll'}(q, \alpha_m) &= V_{ll'}(q) + \psi_{ll'}(q) D(\alpha_m) \\ &\quad + \sum_{l_1} \psi_{ll_1}(q) D(\alpha_m) Q(q, \alpha_m) v_{l_1 l'}(q, \alpha_m) \\ &\quad + \sum_{l_1} V_{ll_1} Q(q, \alpha_m) v_{l_1 l'}(q, \alpha_m), \end{aligned} \quad (2.23)$$

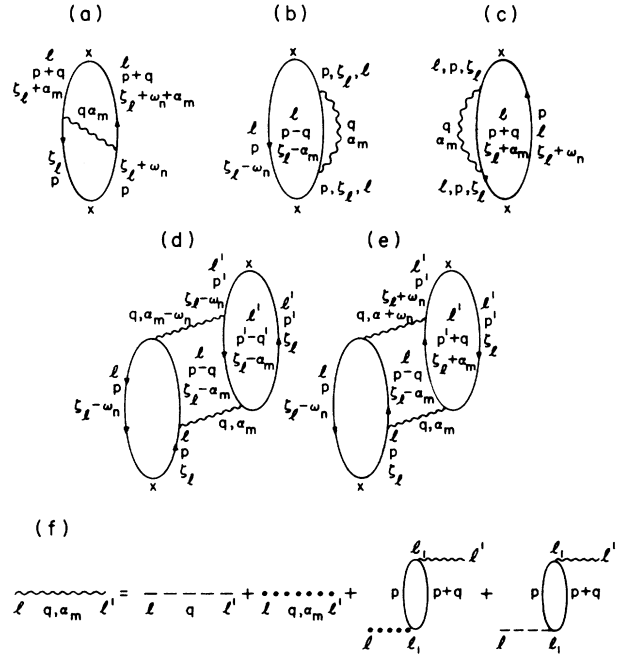


FIG. 1. (a)–(e) The class of diagrams which contribute the high-frequency conductivity (f). Effective interaction is shown.

where

$$\psi_{ll'}(q) = \frac{2\pi e^2}{q} \omega_{LO} \left[\frac{1}{\epsilon_\infty} - \frac{1}{\epsilon_0} \right] e^{-q|l-l'|a}. \quad (2.24)$$

Now the integral equation (2.23) can be solved by Fourier transformation (note $v_{ll'}$ only depend on $l-l'$):

$$v(q, k_z, \alpha_m) = \sum_{l'} v_{ll'}(q, \alpha_m) e^{ik_z(l-l')a}. \quad (2.25)$$

We obtain

$$v(q, k_z, \alpha_m) = \frac{V_q S(q, k_z) + \psi(q, k_z) D(\alpha_m)}{1 - Q(q, \alpha_m) [V_q S(q, k_z) + \psi(q, k_z) D(\alpha_m)]}, \quad (2.26)$$

where

$$\psi(q, k_z) = \frac{2\pi e^2}{q} S(q, k_z) \omega_{LO} \left[\frac{1}{\epsilon_\infty} - \frac{1}{\epsilon_0} \right] \quad (2.27)$$

and

$$S(q, k_z) = \frac{\sinh(qa)}{\cosh(qa) - \cos(k_z a)}. \quad (2.28)$$

Let us define a dielectric function

$$\epsilon(q, \alpha_m) = 1 - V_q Q(q, \alpha_m) S(q, k_z) \quad (2.29)$$

and the “true” phonon propagator

$$\begin{aligned}\tilde{D}(\alpha_m) &= \frac{D(\alpha_m)}{1 - \frac{\psi(q, k_z) D(\alpha_m) Q(q, \alpha_m)}{\epsilon(q, \alpha_m)}} \\ &= \frac{\omega_{LO}}{\alpha_m^2 - \omega_{LO}^2 - \frac{\omega_{LO} \psi(q, k_z) Q(q, \alpha_m)}{\epsilon(q, \alpha_m)}}.\end{aligned}\quad (2.30)$$

Therefore,

$$v(q, \alpha_m) = \frac{V_q S(q, k_z)}{\epsilon(q, \alpha_m)} + \frac{\psi(q, k_z) \tilde{D}(\alpha_m)}{\epsilon(q, \alpha_m)^2}.\quad (2.31)$$

Thus we express our effective interaction by two terms. The first term is the screened Coulomb potential due to the collective motion of the electrons. The second term represents the renormalized phonon interaction at a vertex

with the electron through a screened phonon-electron interaction $\psi(q, \alpha_m)/\epsilon(q, \alpha_m)$. After some algebra, our final result for conductivity reads

$$\sigma(\omega) = \sigma^0(\omega) + \sigma^1(\omega) = \sigma^0(\omega) \left[1 - \frac{1}{\omega} I(\omega) \right],\quad (2.32)$$

where

$$\begin{aligned}I(\omega) &= \frac{\pi}{nm\omega} \int q^3 dq \int \frac{a dk_z}{2\pi} \frac{\psi(q, k_z)}{V_q S(q, k_z)} \\ &\quad \times \frac{i}{2\pi} \text{P} \int dx \coth \left[\frac{\beta x}{2} \right] F(q, x, \omega),\end{aligned}\quad (2.33)$$

where

$$\begin{aligned}F(q, x, \omega) &= [\tilde{D}(x) - \tilde{D}^*(x)] \frac{1}{\epsilon(q, x + \omega)} + \left[\frac{1}{\epsilon(q, x)} - \frac{1}{\epsilon^*(q, x)} \right] \tilde{D}(x + \omega) - \left[\frac{\tilde{D}(x)}{\epsilon(q, x)} - \frac{\tilde{D}^*(x)}{\epsilon^*(q, x)} \right] \\ &\quad - \frac{\psi(q, k_z)}{V_q S(q, k_z)} \left[\frac{\tilde{D}(x + \omega)}{\epsilon(q, x + \omega)^2} [\tilde{D}(x) - \tilde{D}^*(x)] + \tilde{D}(x + \omega) \left[\frac{\tilde{D}(x)}{\epsilon(q, x)^2} - \frac{\tilde{D}^*(x)}{\epsilon^*(q, x)^2} \right] \right. \\ &\quad \left. - \frac{2\tilde{D}(x + \omega)}{\epsilon(q, x + \omega)} \left[\frac{\tilde{D}(x)}{\epsilon(q, x)} - \frac{\tilde{D}^*(x)}{\epsilon^*(q, x)} \right] \right].\end{aligned}\quad (2.33')$$

Here P stands for principal value and

$$f(x) \rightarrow f(x + i\eta) \quad (\eta \rightarrow 0).\quad (2.34)$$

Equation (2.33) is the exact expression in which we have used the fact that Q depends only on absolute value of q and that $\sigma_{\mu\nu}(\omega) = \delta_{\mu\nu} \sigma(\omega)$ for isotropic system. This result is rather complicated, but in principle can be evaluated analytically or numerically for specific problem. The result is applicable both for classical and quantum plasmas for any temperatures, where the average potential energy of interaction per particle should be less than the average kinetic energy.

III. RELAXATION TIME AND RESISTIVITY

The collision process is described by the real part of the conductivity as written in Eqs. (2.32) and (2.33). We see immediately that the only absorption is from the electron-phonon scattering. The phonon propagator \tilde{D} plays an important role in our result. The dispersion relation of the coupled plasmon-LO-phonon modes is given by the poles of \tilde{D} . By using Eqs. (2.27), (2.29), and $\omega_{TO}^2 = \epsilon_\infty / \epsilon_0 \omega_{LO}^2$, we may write \tilde{D} in the following form:

$$\tilde{D}(\omega) = \frac{\omega_{LO} \epsilon(q, \omega)}{(\omega^2 - \omega_{LO}^2 + i\delta\omega) - (\omega^2 - \omega_{TO}^2 + i\delta\omega) \frac{2\pi e^2}{q \epsilon_\infty} Q(q, \omega) S(q, k_z)},\quad (3.1)$$

where ω_{TO} is the transverse-optical-phonon frequency. Here δ is the half width of the free phonon.³⁵ We find that the poles of the dressed phonon propagator are identical to the roots of the dielectric function given by

$$\tilde{\epsilon}(q, \omega) = \epsilon_\infty \frac{\omega^2 - \omega_{LO}^2 + i\delta\omega}{\omega^2 - \omega_{TO}^2 + i\delta\omega} - \frac{2\pi e^2}{q} Q(q, \omega) S(q, k_z).\quad (3.2)$$

In our later numerical work we shall use Eq. (3.1) for our calculation of F of Eq. (2.33'). Let us rewrite Eq. (2.30) as

$$\sigma(\omega) = \sigma^0 \left[\frac{1}{1 + \frac{I/\omega}{1 - I/\omega}} \right].\quad (3.3)$$

The high-frequency limit is given by the condition

$|I(\omega)| \ll \omega$, and we thus obtain the approximate expression for the conductivity

$$\sigma(\omega) = \frac{\sigma^0}{1 + \frac{I_1(\omega) + iI_2(\omega)}{\omega}}. \quad (3.4)$$

Here I_1 and I_2 are, respectively, the real and imaginary parts of $I(\omega)$. The relaxation time and effective mass are related to conductivity by the Drude formula:

$$\sigma(\omega) = \frac{ine^2}{m^* \left[\omega + \frac{i}{\tau} \right]}, \quad (3.5)$$

We find the effective mass

$$m^* = m \left[1 + \frac{I_1(\omega)}{\omega} \right] \quad (3.6)$$

and the relaxation time

$$\tau^{-1} = I_2(\omega). \quad (3.7)$$

Here only linear corrections due to I_1 and I_2 are retained. However, using Eq. (3.3) we obtain for the general case the result

$$\frac{m^*}{m} = \frac{1}{\left[1 + \frac{I_1}{\omega} \right] \left[1 + \frac{I_2^2}{(\omega + I_1)^2} \right]} \quad (3.8)$$

and

$$\tau^{-1} = \frac{I_2}{1 + \frac{I_1}{\omega}}. \quad (3.9)$$

Using the analytical properties of Q , \tilde{D} , and the dielectric function, respectively, we can write

$$\frac{1}{\tau} = \frac{1}{\omega nm} \int q^3 dq \int_{-\pi}^{\pi} \frac{d\theta}{2\pi} \psi(q, \theta) \frac{P}{2} \int dx \left[\coth \frac{\beta x}{2} - \coth \frac{\beta(x+\omega)}{2} \right] F(x, x+\omega), \quad (3.10)$$

where $\theta = ak_z$ and

$$F(x, x+\omega) = F_1(x, x+\omega) - F_2(x, x+\omega), \quad (3.11)$$

with

$$F_1(x, x+\omega) = \frac{2}{V_q S(q, k_z)} \left[\text{Im} \tilde{D}(x) \text{Im} \frac{1}{\epsilon(x+\omega)} + \text{Im} \tilde{D}(x+\omega) \text{Im} \frac{1}{\epsilon(x)} \right] \quad (3.12)$$

and

$$F_2(x, x+\omega) = \frac{2\psi(q, k_z)}{[V_q S(q, k_z)]^2} \left[\text{Im} \frac{\tilde{D}(x+\omega)}{\epsilon(x+\omega)^2} \text{Im} \tilde{D}(x) + \text{Im} \frac{\tilde{D}(x)}{\epsilon(x)^2} \text{Im} \tilde{D}(x+\omega) - 2 \text{Im} \frac{\tilde{D}(x)}{\epsilon(x)} \text{Im} \frac{\tilde{D}(x+\omega)}{\epsilon(x+\omega)} \right]. \quad (3.13)$$

The leading term at high frequencies is given by F_1 . F_2 will contribute terms to the conductivity or absorption which are smaller by a factor ω^{-2} with respect to those obtained from F_1 . We observe that F_2 represents simultaneous excitation of two phonon with a large shift in their energy which makes a small contribution to the conductivity at *high frequencies*. Even at frequencies $\omega \approx \omega_{LO}$ our numerical calculations indicate that the contribution from F_2 is still very small. Therefore, we neglect the contributions from F_2 . Equation (3.10) with Eq. (3.12) is our general result for the absorption which includes the effect of finite lifetime of the phonons. It is apparent that instead of having a δ -function behavior for $\text{Im} D(\bar{x})$, we have here a Lorentzian-like shape. This amounts to an average of the electron density fluctuation $[\text{Im}(1/\epsilon)]$ over a range of frequencies of width $|\Gamma_q^{-1}|$. For the purpose of the calculation we would like to use the following dimensionless variables,

$$z = \frac{q}{2k_F}, \quad \Omega = \frac{\omega}{4E_F}, \quad X = \frac{x}{4E_F}, \quad \Theta = \frac{1}{4E_F\beta}, \quad D' = 4E_F\tilde{D}, \quad Q' = \frac{2\pi e^2}{q\epsilon_\infty} Q, \quad F' = 4E_F \frac{2\pi e^2}{q\epsilon_\infty} F,$$

where E_F is the Fermi energy for electrons. By this we get

$$\frac{1}{\tau} = \frac{8\pi^2\omega_{LO}}{\Omega} \left[1 - \frac{\epsilon_\infty}{\epsilon_0} \right] \int_{-\pi}^{\pi} \frac{d\theta}{2\pi} \int_0^\infty z^3 dz S(z, \theta) \frac{P}{2} \int_{-\infty}^\infty dX \left[\coth \left[\frac{X}{2\Theta} \right] - \coth \left[\frac{X+\Omega}{2\Theta} \right] \right] F'(X, \Omega+X). \quad (3.14)$$

For the case $kT \ll E_F$, we can use the limit ($T \rightarrow 0$) and get

$$\frac{1}{\tau} = \frac{8\pi^2\omega_{LO}}{\Omega} \left[1 - \frac{\epsilon_\infty}{\epsilon_0} \right] \int_{-\pi}^{\pi} \frac{d\theta}{2\pi} \int_0^\infty z^3 dz S(z, \theta) \int_0^\Omega dX F'(X, \Omega-X). \quad (3.15)$$

We will evaluate his inverse collision time numerically for GaAs-Ga_{1-x}Al_xAs and PbTe-Pb_{1-x}Sn_xTe systems.

IV. DISCUSSIONS

In this paper, we have calculated the high-frequency conductivity and relaxation time for superlattice system made out polar or partially polar semiconductors. Here we treat electron-LO-phonon scattering as the dominant scattering mechanism which contribute to the absorption. Our general expression for dynamical conductivity is given in Eqs. (2.32) and (2.33). The conductivity depends on the dressed phonon propagator \tilde{D} which is defined in Eq. (3.1). The poles of \tilde{D} are identical to the roots which determine the phonon-plasma-coupled frequencies [see Eq. (3.2)]. Essentially the same result indicate that the bulk conductivity depends on \tilde{D} rather than D was derived long ago by Ron and Tzoar.³⁶ However, the first calculation that demonstrated the difference of using \tilde{D} rather than D was given by Katayama and co-workers.³⁵ Our calculations indicate that for weak electron-phonon coupling, for semiconductors such as GaAs-Ga_{1-x}Al_xAs, the intensity of \tilde{D} resides almost exclusively in the vicinity of the longitudinal-optic-phonon frequency. In this case using D rather than \tilde{D} in our expression for the conductivity should yield a realistic approximation for the conductivity. Our numerical results indicate it to be true.

For the case of strong electron-phonon coupling, for materials such as PbTe-Pb_{1-x}Sn_xTe, the intensity of \tilde{D} shows two broad resonances which can be identified as “dressed phonon” and “dressed plasmon.” We find significant difference in our results if we use D rather than \tilde{D} in our expression for the conductivity. We thus may conclude that for polar material having strong electron-phonon coupling the dressed phonon propagator should be used.

In our figures we have plotted the real part of the conductivity and the inverse collision time as a function of the normalized frequency. From the real part of the conductivity, one can see clearly the scattering from two coupled modes. However, for the inverse collision time the peak at low frequency is drastically reduced. This comes about since the inverse collision time is proportional to $\omega^2\sigma_1$, and the peak is at frequency ω_0 which is smaller than its effective width. Thus the factor ω^2 strongly suppresses the resonant effect for τ^{-1} at ω_0 . In Fig. 2 we plot the numerical results of the real part of the conductivity and the inverse collision time (τ^{-1}) for weakly polar material (GaAs-Ga_{1-x}Al_xAs). The difference between using the bare phonon propagator rather than the dressed phonon propagator is small. The absorption at frequencies below the LO-phonon frequency is not noticeable for the case of weak electron-phonon coupling. We note, however, that the absorption at ω larger than ω_{LO} is re-

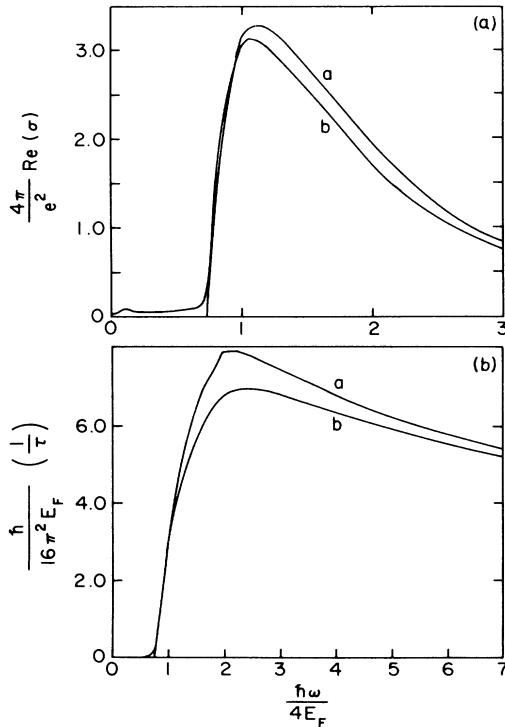


FIG. 2. Plot of (a) $\text{Re}(\sigma)$ and (b) τ^{-1} as a function of normalized frequency Ω for GaAs-Ga_{1-x}Al_xAs, where $n_s=3.6 \times 10^{11} \text{ cm}^{-2}$, $\delta=0.004E_F$, and $a=0.5 \times 10^{-6} \text{ cm}$. (a) shows bare phonon scattering; (b) shows coupled mode scattering.

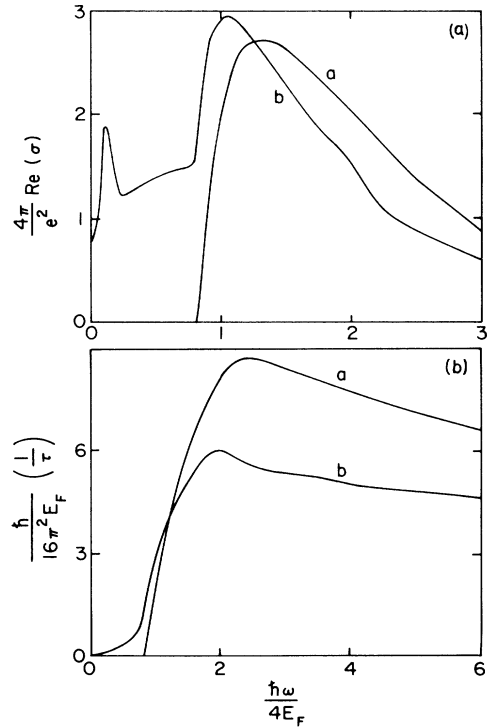


FIG. 3. Plot of (a) $\text{Re}(\sigma)$ and (b) τ^{-1} as a function of normalized frequency Ω for PbTe-Pb_{1-x}Sn_xTe, where $n_s=3.6 \times 10^{11} \text{ cm}^{-2}$, $\delta=0.01E_F$, and $a=0.5 \times 10^{-6} \text{ cm}$. (a) shows bare phonon scattering; (b) shows coupled mode scattering.

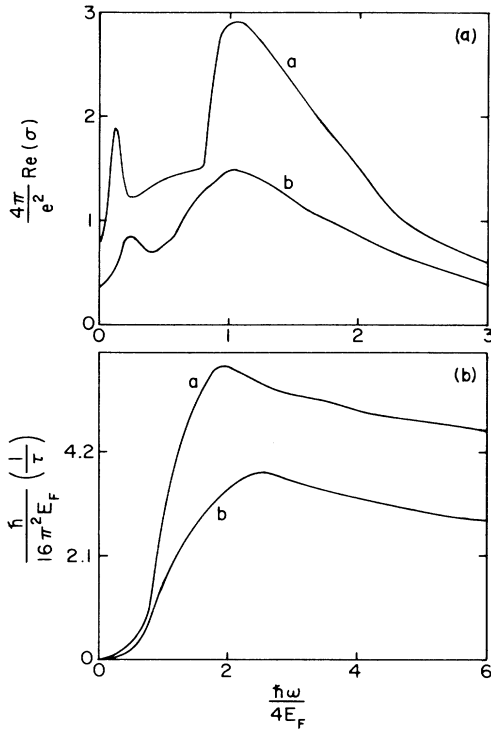


FIG. 4. Plot of (a) $\text{Re}(\sigma)$ and (b) τ^{-1} as a function of normalized frequency Ω for $\text{PbTe-Pb}_{1-x}\text{Sn}_x\text{Te}$. (a) $n_s = 3.6 \times 10^{11} \text{ cm}^{-2}$, $\delta = 0.01E_F$, and $a = 0.5 \times 10^{-6} \text{ cm}$. (b) $n_s = 7.6 \times 10^{11} \text{ cm}^{-2}$, $\delta = 0.01E_F$, and $a = 1.0 \times 10^{-6} \text{ cm}$. The x coordinate is $\omega/4E_F$, where E_F is the value calculated by using $n_s = 3.6 \times 10^{11} \text{ cm}^{-2}$.

duced for the dressed phonon in comparison with the bare phonon, just as has been reported for the bulk case.³⁵ In Fig. 3 we present our numerical results for the real part of conductivity and inverse collision time for $\text{PbTe-Pb}_{1-x}\text{Sn}_x\text{Te}$, which is a strongly interacting electron-phonon system. In this case, we found a large difference in the real part of conductivity as well as in the inverse collision time between the bare phonon scattering and the dressed phonon scattering. For the case of strong electron-phonon coupling the peak in real part of conductivity at low frequencies is due to the scattering from the low-lying mode in the density fluctuation of the electron-phonon system. In Fig. 4 the lower curve is obtained by changing $a \rightarrow 2a$, $n \rightarrow 2n$ (n/a is a constant, i.e., the volume density is fixed). Under this change both the real part of conductivity and the inverse collision time are greatly reduced due to the increasing in screening and decreasing in coupling between layers. In Fig. 5 we present

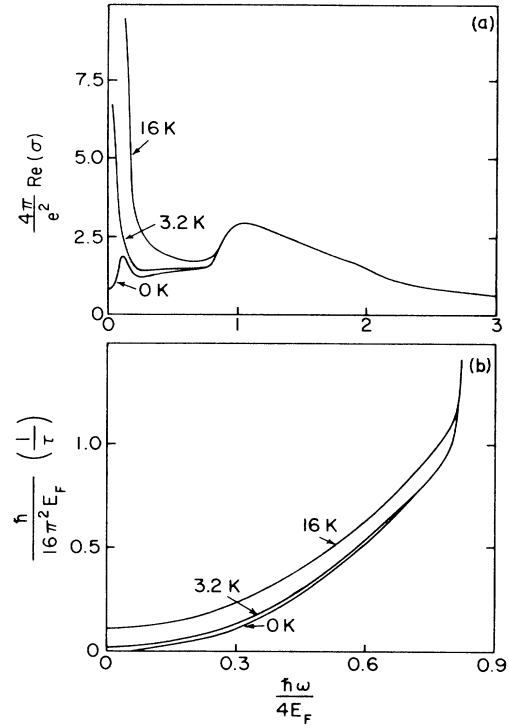


FIG. 5. Plot of (a) $\text{Re}(\sigma)$ and (b) τ^{-1} as a function of normalized frequency Ω for $\text{PbTe}_{1-x}\text{Sn}_x\text{Te}$ for three different temperatures, where $n_s = 3.6 \times 10^{11} \text{ cm}^{-2}$, $\delta = 0.01E_F$, and $a = 0.5 \times 10^{-6} \text{ cm}$.

our numerical results for the real part of the conductivity and the inverse collision time for $\text{PbTe-Pb}_{1-x}\text{Sn}_x\text{Te}$ with the same parameters as in Fig. 3. Here, for finite temperature, τ^{-1} is finite in the small frequency limit, and the real part of the conductivity is greatly increased in this regime. The physical parameters used in our calculation are the following: $\epsilon_0^{\text{PbTe}} = 1333.0$, $\epsilon_\infty^{\text{PbTe}} = 33.0$, $\omega_{\text{LO}}^{\text{PbTe}} = 13.4 \text{ meV}$, $m^{\text{PbTe}} = 0.21m_0$, $\epsilon_0^{\text{GaAs}} = 12.5$, $\epsilon_\infty^{\text{GaAs}} = 10.8$, $\omega_{\text{LO}}^{\text{GaAs}} = 36 \text{ meV}$, $m^{\text{GaAs}} = 0.07m_0$, where m_0 is the free-electron mass.

In conclusion, we have calculated the high-frequency conductivity of superlattice system with electron-LO-phonon interaction. General result has been derived in terms of integral and numerical computation has been done for some typical parameters for type-I superlattices. We note that our work can be easily generalized to calculate, say, the collision frequency due to phonon of the electron and the holes, respectively, for type-II superlattices.

¹For the recent work on superlattices, see Proceedings of Fifth International Conference on Electronic Properties of Two-dimensional Systems, Oxford, 1983 [Surf. Sci. **142**, (1984)].

²For an excellent review of the subject, see the review article by T. Ando, A. B. Fowler, and F. Stern, Rev. Mod. Phys. **54**,

437 (1982).

³R. Dingle, H. L. Stormer, A. C. Gossard, and W. Wiegmann, Surf. Sci. **98**, 90 (1980).

⁴L. L. Chang and L. Esaki, Surf. Sci. **98**, 70 (1980).

⁵S. Das, Sarma and J. J. Quinn, Phys. Rev. B **25**, 7603 (1982).

- ⁶A. C. Tselis and J. J. Quinn, *Phys. Rev. B* **29**, 3318 (1984).
⁷L. L. Chang, *Surf. Sci.* **73**, 226 (1978).
⁸R. Dingle, *Surf. Sci.* **73**, 229 (1978).
⁹A. Pinczuk, J. M. Worlock, H. L. Stormer, R. Dingle, W. Wiegmann, and A. C. Gossard, *Solid State Commun.* **36**, 43 (1980).
¹⁰G. Abstreiter, Ch. Zeller, and K. Plong, in *Gallium Arsenide and Related Compounds*, edited by H. W. Thim (Institute of Physics, Bristol, 1980), p. 741.
¹¹P. Manuel, G. A. Sai-Halasz, L. L. Chang, C. A. Chang, and L. Esaki, *Phys. Rev. Lett.* **37**, 1701 (1976).
¹²Jainendra K. Jain and Philip B. Allen, *Phys. Rev. Lett.* **54**, 947 (1984).
¹³W. A. Harrison, *J. Vac. Sci. Technol.* **14**, 1016 (1977).
¹⁴G. A. Sai-Halasz, R. Tsu, and L. Esaki, *Appl. Phys. Lett.* **30**, 651 (1977).
¹⁵G. A. Sai-Halasz, L. Esaki, and W. A. Harrison, *Phys. Rev. B* **18**, 2812 (1978).
¹⁶A. Madhukar, N. V. Dandekar, and R. N. Nucho, *J. Vac. Sci. Technol.* **16**, 1507 (1979).
¹⁷N. Tzoar and C. Zhang, *Phys. Rev. B* **32**, 1149 (1985).
¹⁸N. Tzoar and C. Zhang, *Phys. Rev. B* **33**, 2624 (1986).
¹⁹S. Das Sarma and B. A. Mason, *Ann. Phys.* **163**, 78 (1985).
²⁰S. Das Sarma and A. Madhukar, *Phys. Rev. B* **22**, 2823 (1980).
²¹G. Kawamoto, J. J. Quinn, and W. L. Bloss, *Phys. Rev. B* **23**, 1875 (1981); T. S. Rahman, D. L. Mills, and P. S. Riseborough, *ibid.* **23**, 4081 (1981).
²²P. J. Price, *Ann. Phys.* **133**, 217 (1981); *Surf. Sci.* **113**, 199 (1982).
²³D. K. Ferry, *Surf. Sci.* **75**, 86 (1978); K. Hess, *Appl. Phys. Lett.* **35**, 484 (1979); P. K. Basu and B. R. Nag, *Phys. Rev. B* **22**, 4849 (1980).
²⁴S. Das Sarma, *Phys. Rev. B* **27**, 2590 (1983).
²⁵S. Das Sarma, *Phys. Rev. Lett.* **52**, 859 (1984).
²⁶G. Lindemann, W. Seidebusch, R. Lassnig, J. Edlinger, and E. Gornik, *Physica* **117&118B**, 649 (1983).
²⁷D. C. Tsui, Th. Englert, A. Y. Cho, and A. C. Gossard, *Phys. Rev. Lett.* **44**, 341 (1980); G. Kido, N. Miura, H. Ohno, and H. Sakaki, *J. Phys. Soc. Jpn.* **51**, 2168 (1982).
²⁸J. Scholz, F. Koch, J. Zeigler, and H. Maier, *Solid State Commun.* **46**, 665 (1983).
²⁹Th. Englert, J. C. Maan, Ch. Uihlein, D. C. Tsui, and A. C. Gossard, *Solid State Commun.* **46**, 545 (1983).
³⁰M. A. Brummel, R. J. Nicholas, J. C. Portal, M. Razeghi, and M. A. Poisson, *Physica* **117&118B**, 753 (1983).
³¹M. Horst, U. Merkt, and J. P. Kotthaus, *Phys. Rev. Lett.* **50**, 754 (1983).
³²A. Pinczuk and J. M. Worlock, *Physica* **117&118B**, 637 (1983).
³³R. Kubo, *J. Phys. Soc. Jpn.* **12**, 570 (1957).
³⁴See, for example, A. Ron and N. Tzoar, *Phys. Rev.* **131**, 12 (1963).
³⁵S. Katayama, D. L. Mills, and R. Sirko, *Phys. Rev. B* **28**, 6079 (1983); S. Katayama and D. L. Mills, *ibid.* **19**, 6513 (1979).
³⁶A. Ron and N. Tzoar, *Phys. Rev.* **133**, A1378 (1963).
³⁷J. Appel and A. W. Overhauser, *Phys. Rev. B* **10**, 758 (1978); N. Tzoar and P. M. Platzman, *ibid.* **20**, 4189 (1979).